

## Effect of minor Sc and Zr on superplasticity of Al-Mg-Mn alloys

PENG Yong-yi(彭勇宜)<sup>1,2</sup>, YIN Zhi-min(尹志民)<sup>1</sup>, NIE Bo(聂波)<sup>1,3</sup>, ZHONG Li(钟利)<sup>1,3</sup>

1. School of Materials Science and Engineering, Central South University, Changsha 410083, China;

2. School of Physics Science and Technology, Central South University, Changsha 410083, China;

3. Northeast Light Alloy Co. Ltd., Harbin150060, China

Received 18 June 2007; accepted 16 July 2007

**Abstract:** The effect of Sc and Zr on the superplastic properties of Al-Mg-Mn alloy sheets was investigated by control experiment. The superplastic properties and the mechanism of superplastic deformation of the two alloys were studied by means of optical microscope, scanning electronic microscope and transmission electron microscope. The elongation to failure of Al-Mg-Mn-Sc-Zr alloy is larger than that of Al-Mg-Mn alloy at the same temperature and initial strain rate. The variation of strain rate sensitivity index is similar to that of elongation to failure. In addition, Al-Mg-Mn-Sc-Zr alloy exhibits higher strain rate superplastic property. The activation energies of the two alloys that are calculated by constitutive equation and linear regression method approach the energy of grain boundary diffusion. The addition of Sc and Zr decreases activation energy and improves the superplastic property of Al-Mg-Mn alloy. The addition of Sc and Zr refines the grain structure greatly. The main mechanism of superplastic deformation of the two alloys is grain boundary sliding accommodated by grain boundary diffusion. The fine grain structure and high density of grain boundary, benefit grain boundary sliding, and dynamic recrystallization brings new fine grain and high angle grain boundary which benefit grain boundary sliding too. Grain boundary diffusion, dislocation motion and dynamic recrystallization harmonize the grain boundary sliding during deformation.

**Key words:** Sc; Zr; Al-Mg-Mn alloy; superplasticity; grain boundary sliding; activation energy

### 1 Introduction

Many investigations have shown that the addition of minor Sc, especially the joint addition of minor Sc with minor Zr can remarkably enhance the strength of Al-Mg-Mn alloy[1–2]. The novel Al-Mg-Mn alloy containing minor Sc and Zr is the most promising material for aerospace applications due to its high strength, good corrosion resistance, weldability, and fatigue fracture resistance[3–5]. It is desired to develop non-heat-treated Al-Mg-Mn-Sc-Zr alloy sheets by superplastic forming. The superplastic forming rate is required to be sufficiently high, and the forming temperature is required as low as possible. Only when the strain rate is greater than  $10^{-2} \text{ s}^{-1}$ , can the current industrial fabrication speed be satisfied.

In order to obtain high strain rate and low temperature superplasticity, the method for obtaining ultra-fine grained materials has been recently developed by using severe plastic deformation (SPD), such as

accumulative roll bonding (ARB)[6], equal channel angular pressing (ECAP)[7–8]. Of these, many investigations were focused on Al alloy containing minor Sc and/or Zr. However the exact effect of Sc and/or Zr on the microstructure evolution and the mechanism of superplastic deformation in Al-Mg-Mn alloy were not clear. Different researcher brought forward different mechanism of superplastic deformation for Al-Mg-Mn-Sc-Zr alloy[7, 9–10].

The aim of present work is to investigate the effect of Sc and Zr on the superplasticity of Al-Mg-Mn alloy by control experiment, to quest for the relationship between the microstructure and the mechanism of superplastic deformation.

### 2 Experimental

#### 2.1 Materials

The chemical compositions of the two studied alloys are listed in Table 1. The both alloy ingots were produced by semi-continuous casting technique, then

**Table 1** Chemical compositions of studied alloys (mass fraction, %)

Sample No.	Mg	Mn	Sc	Zr	Al
1	6.2	0.4	0.25	0.12	Bal.
2	6.2	0.4	—	—	Bal.

homogenized, hot rolled, cold-rolled to 2.6 mm-thick sheet successively, and annealed for stabilization in the end.

**2.2 Method**

The gauge dimensions of the tensile specimen were 10 mm×6 mm×2.6 mm. Tensile tests were carried out on Instron 8032 Servo-hydraulic machine equipped with a three-zone furnace at constant crosshead speed. Tensile tests were conducted in air at temperatures between 623 K and 813 K and at initial strain rates between  $1.67 \times 10^{-4} \text{ s}^{-1}$  and  $1.67 \times 10^{-1} \text{ s}^{-1}$ . The accuracy of temperature was controlled within  $\pm 1 \text{ K}$ . The specimens were held for about 15 min at the testing temperature in order to reach thermal equilibrium. Once specimen was pulled to failure, it was quenched into cold water quickly.

The metallurgical microstructure of specimens was investigated by means of optical microscope(OM). The micrographs of fractures were observed by scanning electronic microscope (SEM, SIRION 200). Thin foils for transmission electron microscopy(TEM) were prepared by twin-jet polishing with an electrolyte solution consisting of 4% perchloric acid and 96% absolute alcohol below  $-20^\circ\text{C}$ . The foils were observed on a TECNAI G<sup>2</sup>20 transmission electron microscope.

**3 Results and discussion**

**3.1 Mechanical properties**

The elongations to failure of Al-Mg-Mn alloy with and without Sc and Zr at different temperatures and initial strain rates are shown in Fig.1.

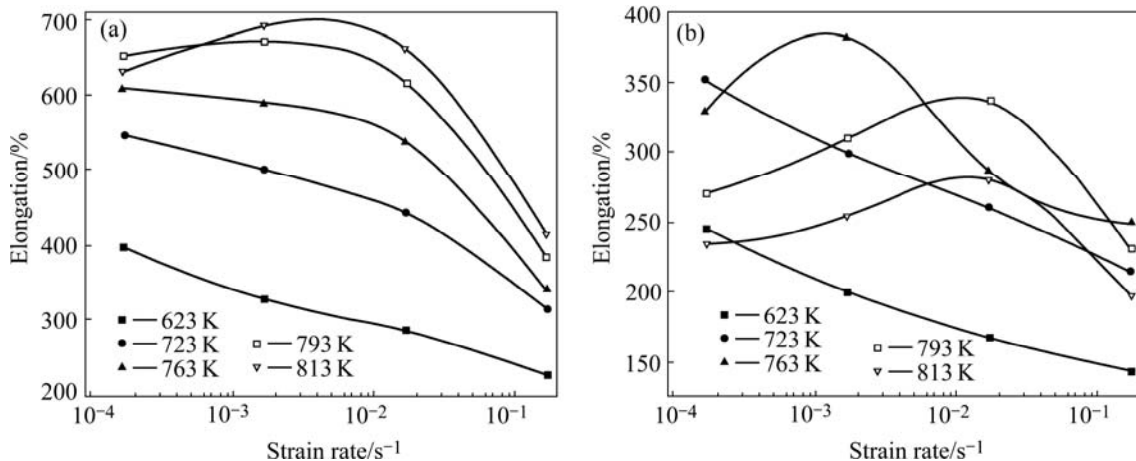


**Fig.1** Elongations to failure of Al-Mg-Mn-Sc-Zr alloy (a) and Al-Mg-Mn alloy (b)

It is seen that the elongations to failure of Al-Mg-Mn-Sc-Zr are higher than those of Al-Mg-Mn alloy at the same temperature and initial strain rate. The maximum elongation to failure of Al-Mg-Mn alloy without minor Sc and Zr is only 382% obtained at 763 K and  $1.67 \times 10^{-3} \text{ s}^{-1}$ , and the maximum elongation to failure of Al-Mg-Mn alloy with minor Sc and Zr is 690% obtained at 793 K and  $1.67 \times 10^{-3} \text{ s}^{-1}$ . For the two alloys, the optimum strain rate has a tendency of increase with the increase of deformation temperature. Meanwhile, Al-Mg-Mn alloy with minor Sc and Zr exhibits superplastic properties at higher strain rate and/or lower deformation temperature.

The fractured specimens of Al-Mg-Mn-Sc-Zr alloy tested at 813 K and various strain rates, the fractured specimens of Al-Mg-Mn alloy tested at 763 K and various strain rates and untested specimen are shown in Fig.2. For Al-Mg-Mn-Sc-Zr alloy, localization deformation and necking are visible in the specimens pulled to failure at  $1.67 \times 10^{-1} \text{ s}^{-1}$ , but very uniform deformation and negligible necking occur in the gauge length of specimens tested at other strain rates.

The typical true stress—true strain curves ( $\sigma-\epsilon$ ) of Al-Mg-Mn alloy with and without Sc and Zr are shown in Fig.3. It is shown that flow stress begins to stabilize, and then gradually falls with strain increasing after initial strain hardening. The relationships of flow stress and strain rate at different temperatures for the two alloys are summarized in the  $\ln \sigma-\ln \dot{\epsilon}$  plot in Fig.4. And the fitted lines obtained by linear regression method at various temperatures are also shown in Fig.4. For the two alloys, at the same temperature, the maximum flow stress increases with the increase of strain rate. At the same time the flow stress decreases with the increase of deformation temperature. In addition, the Al-Mg-Mn-Sc-Zr alloy exhibits lower flow stresses than Al-Mg-Mn alloy at the same temperature and initial strain rate.

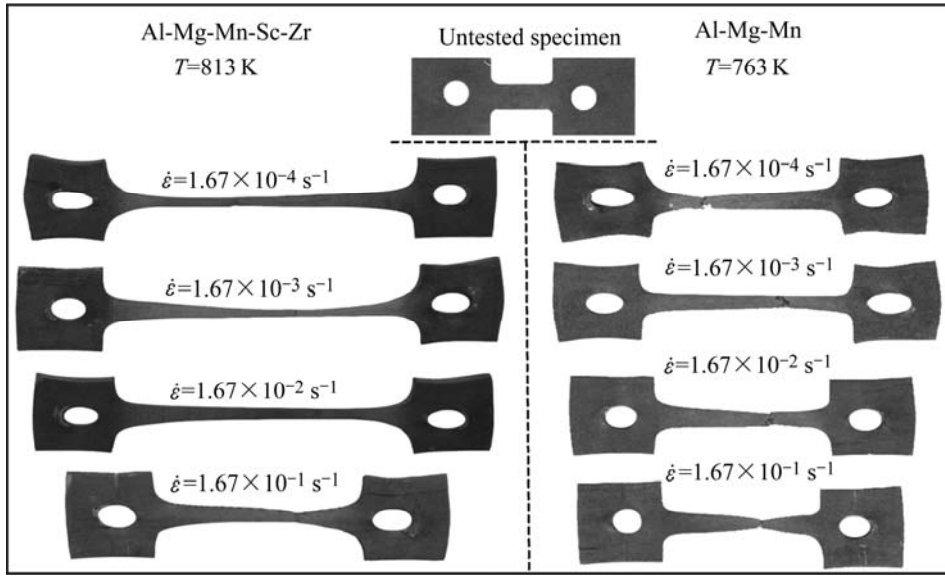


Fig.2 Appearance of untested specimen and some specimens pulled to failure

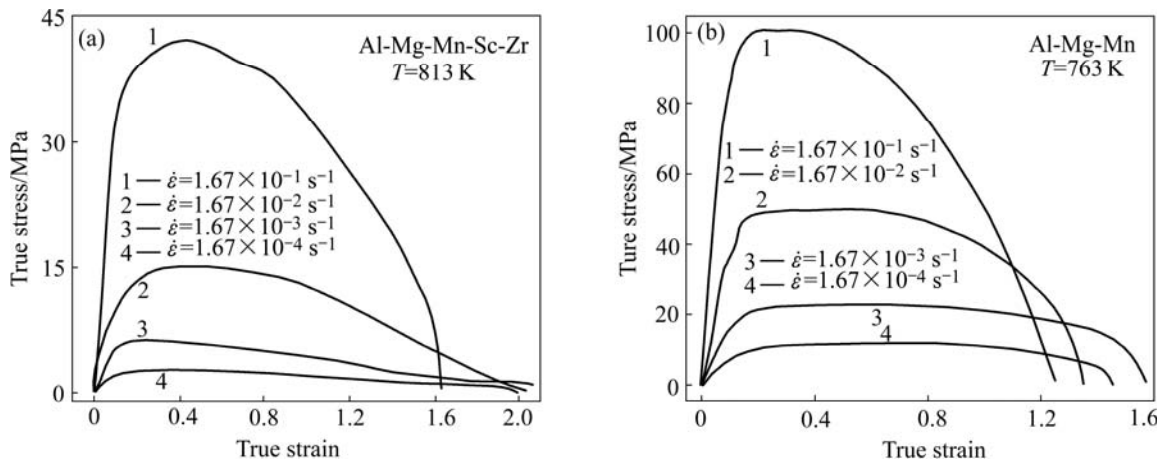


Fig.3 True stress—true strain curves of two alloys

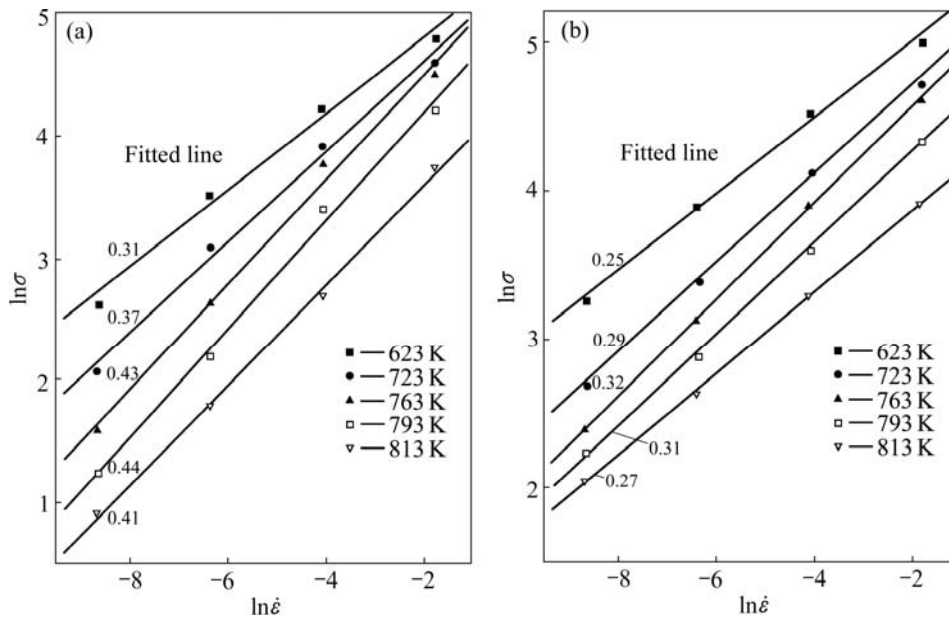


Fig.4  $\ln \sigma$ — $\ln \dot{\epsilon}$  plots of two alloys at different temperatures: (a) Al-Mg-Mn-Sc-Zr; (b) Al-Mg-Mn

**3.2 Strain rate sensitivity index and activation energy**

To obtain a clear understanding of the above features, the strain rate sensitivity index  $m$  and the activation energies of the two alloys are calculated according to the following constitutive equation[7]:

$$\sigma = k[\dot{\epsilon} \exp(Q/(RT))]^m \tag{1}$$

where  $\sigma$  is the flow stress,  $k$  is a material constant,  $\dot{\epsilon}$  is the steady state strain rate,  $Q$  is the activation energy for superplastic deformation,  $R$  is the universal gas constant and  $T$  is absolute temperature.  $Q$  is a definite value at a certain temperature, so the strain rate sensitivity index  $m$  can be expressed by

$$m = \frac{\partial \ln \sigma}{\partial \ln \dot{\epsilon}} \tag{2}$$

Then, the slopes of the fitted lines obtained by linear regression method at various temperatures in the plot of  $\ln \sigma - \ln \dot{\epsilon}$  are the values of  $m$ . From low temperature to high temperature, the strain rate sensitivity index  $m$  of Al-Mg-Mn-Sc-Zr alloy is 0.31, 0.37, 0.43, 0.44 and 0.41 in turn; the  $m$  value of Al-Mg-Mn alloy is 0.25, 0.29, 0.32, 0.31 and 0.27 in turn. At the same temperature, the  $m$  of Al-Mg-Mn-Sc-Zr alloy is greater than that of Al-Mg-Mn alloy. For these two alloys, the variation of  $m$  is similar to that of elongation. In general, higher  $m$  can result in higher tensile elongation. But the maximal  $m$  and the maximal elongation of Al-Mg-Mn-Sc-Zr don't emerge at the same temperature. This phenomenon that the maximal elongation and the maximal  $m$  don't always emerge at the same temperature or same strain rate was reported in Refs.[11–12]. The activation energy under constant strain rate,  $Q$ , can be calculated by the following equation

deduced from Eqn.(1):

$$Q = \frac{R}{m} \frac{\partial \ln \sigma}{\partial (1/T)} \tag{3}$$

The curves of  $\ln \sigma$  versus  $1/T$  can be obtained according to Fig.4.  $\partial \ln \sigma / \partial \ln (1/T)$  is estimated from the slopes of the fitted linear regression lines in Fig.5. The average activation energies of Al-Mg-Mn-Sc-Zr alloy and Al-Mg-Mn alloy are 74.8 and 84.5 kJ/mol, respectively. These results are close to the activation energy of grain boundary diffusion in aluminum alloy, 84 kJ/mol[13–15]. This suggests the dominant mechanism of superplastic deformation is grain boundary sliding accommodated by grain boundary diffusion[16–18]. The grain boundary diffusion plays an important role in superplastic deformation of these two alloys. As a result of the addition of Sc and Zr, the activation energy of Al-Mg-Mn-Sc-Zr alloy is lower than that of Al-Mg-Mn alloy. The lower activation energy weakens the strain hardening effect. This leads to the lower resistance of deformation and larger elongation.

**3.3 Observation of microstructure**

The optical microstructures of the starting materials are shown in Fig.6. The microstructure of Al-Mg-Mn-Sc-Zr alloy has fine unrecrystallization structure, but the microstructure of Al-Mg-Mn alloy is nearly equiaxial coarse recrystallized structure. Dispersive  $Al_3Sc$  and  $Al_3(Sc_{1-x}Zr_x)$  particles in Al-Mg-Mn-Sc-Zr alloy can pin the dislocations and subgrain boundaries strongly[2–3]. The addition of Sc and Zr refines the grain structure of Al-Mg-Mn alloy and restricts grain growth, so Al-Mg-Mn alloy containing Sc and Zr has excellent thermal stability[4]. The fine grain structure makes the microstructure for better superplastic property. It is the

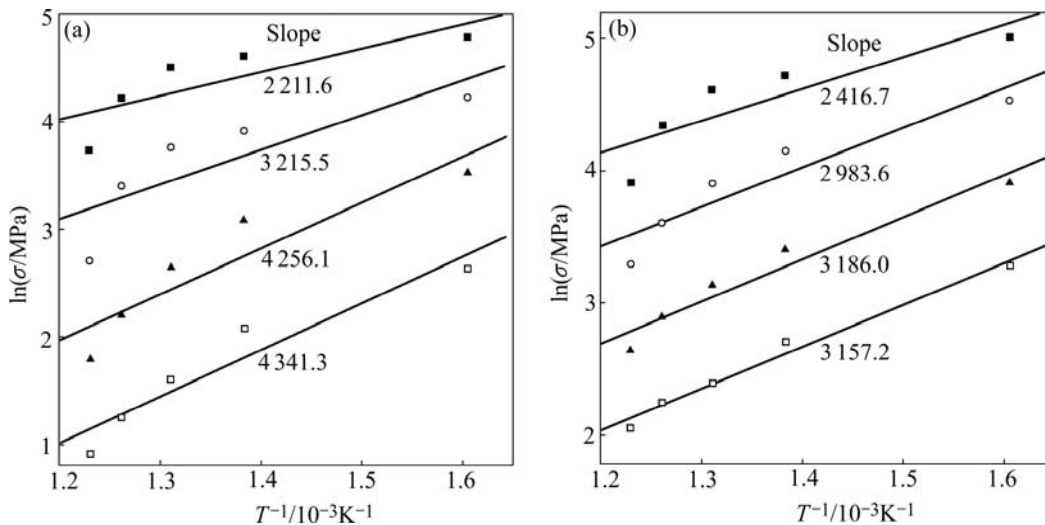


**Fig.5** Fitted curves of  $\ln \sigma - 1/T$  at different strain rates: (a) Al-Mg-Mn-Sc-Zr alloy; (b) Al-Mg-Mn alloy; ■  $1.67 \times 10^{-1} \text{ s}^{-1}$ ; ○  $1.67 \times 10^{-2} \text{ s}^{-1}$ ; ▲  $1.67 \times 10^{-3} \text{ s}^{-1}$ ; □  $1.67 \times 10^{-4} \text{ s}^{-1}$

refined microstructure and the effect of Sc and Zr on the dislocations and subgrain boundaries that cause the excellent superplasticity of Al-Mg-Mn-Sc-Zr alloy at high strain rate ( $\geq 10^{-2} \text{ s}^{-1}$ ) [12, 19–20]. The density of grain boundary in Al-Mg-Mn-Sc-Zr alloy is also higher than that in Al-Mg-Mn alloy. However, at elevated temperature, the grain boundary strength is lower than the grain interior strength. Under the condition of superplastic tensile, the relationship between flow stress  $\sigma$  and grain size  $d$  is  $\sigma \propto d^n$  [21], where  $n$  is a coefficient between 0.7 and 2. Therefore the flow stress of Al-Mg-Mn-Sc-Zr alloy is lower than that of Al-Mg-Mn alloy at

same temperature and strain rate.

Dynamic recrystallization is often found in the course of superplastic deformation. Figs.7(a) and (b) show the typical microstructure of dynamic recrystallization in the two alloys. There are new grain growth and emergence of subgrain. It is notable that some dislocations are pinned by fine  $\text{Al}_3\text{Sc}$  and  $\text{Al}_3(\text{Sc}_{1-x}\text{Zr}_x)$  particles in Figs.7(a) and (c). Although Sc and Zr are strong microstructure stabilizer in Al-Mg-Mn-Sc-Zr alloy, dispersive particles  $\text{Al}_3\text{Sc}$  and  $\text{Al}_3(\text{Sc}_{1-x}\text{Zr}_x)$  can pin dislocation and grain boundary commendably, and dynamic recrystallization and grain

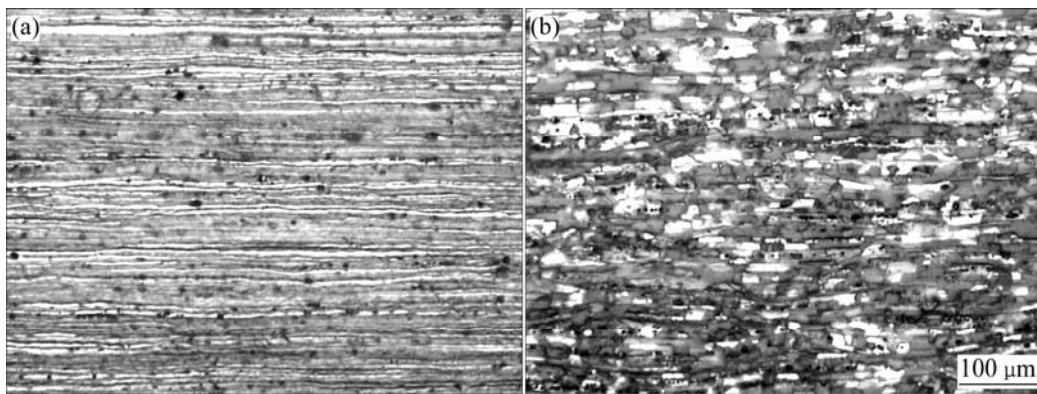


**Fig.6** Microstructures of experimental alloys: (a) Al-Mg-Mn-Sc-Zr alloy; (b) Al-Mg-Mn alloy

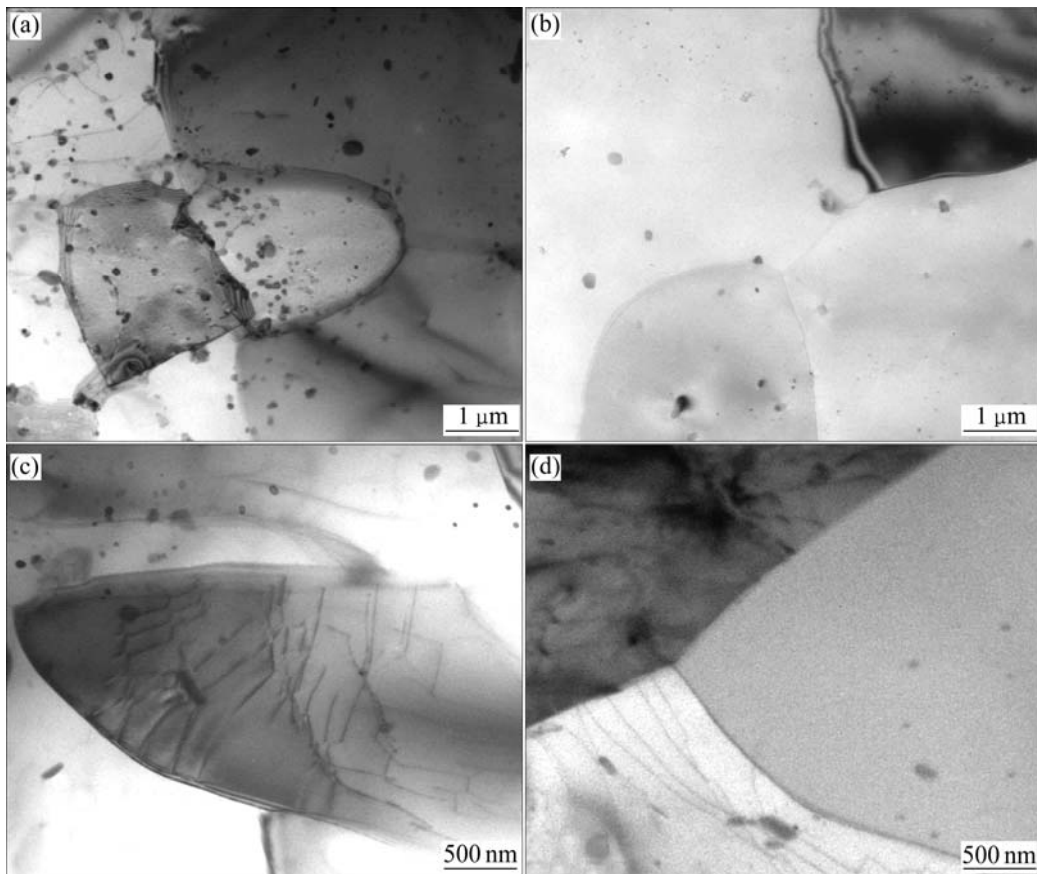


**Fig.7** TEM micrographs of dynamic recrystallization and dislocation motion: (a) Alloy 1 at 763 K and  $1.67 \times 10^{-2} \text{ s}^{-1}$ ; (b) Alloy 2 at 723 K and  $1.67 \times 10^{-3} \text{ s}^{-1}$ ; (c) Alloy 1 at 793 K and  $1.67 \times 10^{-2} \text{ s}^{-1}$ ; (d) Alloy 2 at 793 K and  $1.67 \times 10^{-2} \text{ s}^{-1}$

growth still occur at high temperature. The main mechanism of superplastic deformation is grain boundary sliding (GBS) [15–20]. GBS benefits from dynamic recrystallization, dislocation motion and atomic diffusion. Dislocation always piles at triangle grain boundary along with superplastic deformation increment. Once strain energy is enough, dynamic recrystallization happens. Dynamic recrystallization can deplete ambient distortion energy, decrease dislocation density and relax local stress concentration. And dynamic recrystallization brings new fine grains and new high angle grain boundaries that benefit grain boundary sliding. For Al-Mg-Mn-Sc-Zr alloy, the testing temperature of 623 K is too low for dynamic recrystallization to occur and then less elongations are obtained at all testing strain rates. The elongation at the highest testing temperature of 813 K and strain rate of  $1.67 \times 10^{-4} \text{ s}^{-1}$  is lower than that at testing temperature of 793 K and strain rate of  $1.67 \times 10^{-4} \text{ s}^{-1}$ . This may result from excessive grain growth during deformation. At low strain rate, the deformation time is relatively long for dynamic recrystallization and subsequent grain growth. For Al-Mg-Mn alloy, when the temperature is higher than or equal to 763 K and strain rate is  $1.67 \times 10^{-4} \text{ s}^{-1}$ , excessive grain growth may happen. Its elongations decrease with the increase of temperature. For the both alloys, their elongations at higher strain rates decrease, and dynamic recrystallization doesn't happen due to the short time of deformation. Hence it is difficult for grain boundary to slide.

The grain boundary strength is lower than transgranular strength at elevated temperature. The course of superplastic deformation is similar to the viscous flow. When GBS is impeded during superplastic deformation, stress concentration occurs at grain boundary, triangle grain boundary and the second phase particle. If local stress concentration is greater than or equal to the critical shear stress, GBS and dislocation motion will take place to relax local stress concentration. Figs. 7(c) and (d) show the typical dislocation motion in the two alloys. The surplus dislocations at a grain boundary radiate to interior of grain and vanish at the opposite grain boundary. Sometimes dislocations at interior of grain move to grain boundary. These dislocation motions promote grain boundary sliding, then grain boundary sliding becomes easy. Additionally, diffusional creep can also accelerate dislocation climb and relax stress concentration at low strain rate. There are lots of high angle grain boundaries in finer grained structure. Grain boundary sliding in Al-Mg-Mn-Sc-Zr alloy is easier to happen than in Al-Mg-Mn alloy. Accordingly, Al-Mg-Mn-Sc-Zr alloy obtain larger elongations during superplastic deformation.

Fig. 8 shows the typical SEM micrographs of fractures of the two alloys. Many fine grains can be seen in Figs. 8(a) and (b). The fractures of the two kinds of alloys are mainly intergranular type, and there are a few dimples and tear ridges. Although the local stress concentration can be harmonized by grain boundary diffusion and dislocation motion, cavity nucleates and

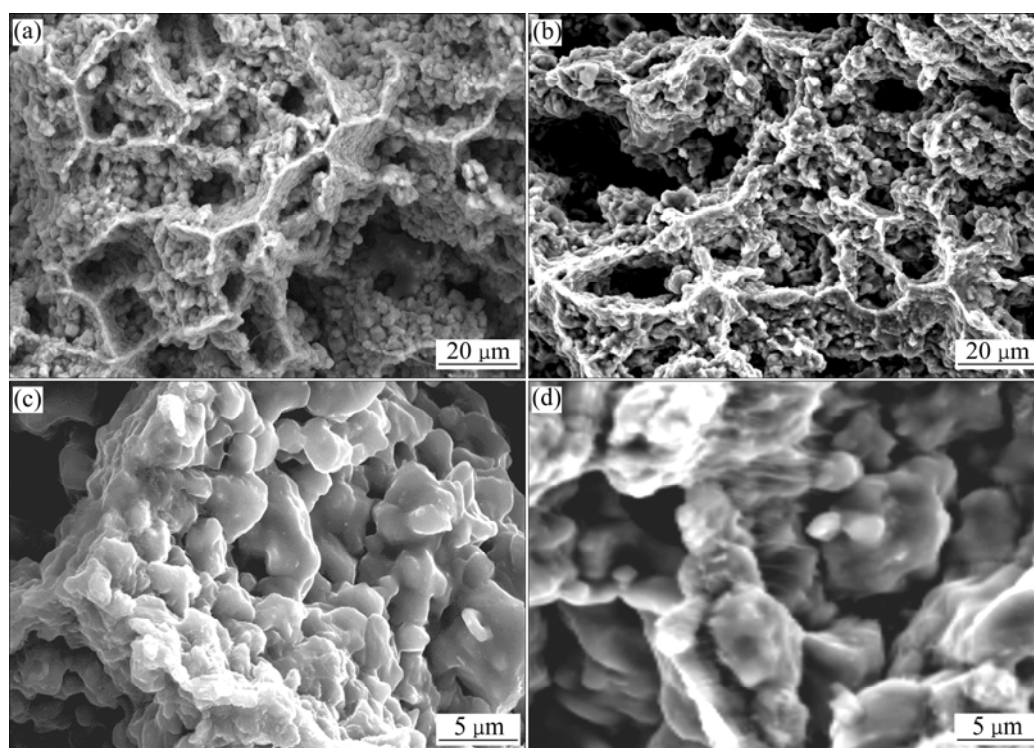


**Fig. 8** SEM images of fracture of two alloys: (a) Alloy 1 at 763 K and  $1.67 \times 10^{-1} \text{ s}^{-1}$ ; (b) Alloy 2 at 763 K and  $1.67 \times 10^{-2} \text{ s}^{-1}$ ; (c) Alloy 1 at 793 K and  $1.67 \times 10^{-1} \text{ s}^{-1}$ ; (d) Alloy 2 at 793 K and  $1.67 \times 10^{-2} \text{ s}^{-1}$

grows at grain boundary and at the second phase particles, especially at triangle grain boundary when the speed of grain boundary sliding exceeds the speed of harmonization. Thus, the connection and growth of dimples can be found in Figs.8(a) and (b). At higher temperature, the grains at fractures of the two alloys are nearly equiaxial grains (Figs.8(c) and (d)), and the fractures are obvious intergranular type. These characteristics of fractures further show that the main mechanism of superplastic deformation for the both alloys is grain boundary sliding [22–23].

## 4 Conclusions

1) The addition of minor Sc and Zr can improve the superplastic property of Al-Mg-Mn alloy. The elongation to failure of Al-Mg-Mn alloy with Sc and Zr is larger than that of Al-Mg-Mn alloy without Sc and Zr at the same temperature and initial strain rate. In addition, Al-Mg-Mn alloy with minor Sc and Zr exhibits higher strain rate superplastic properties.

2) The activation energies of Al-Mg-Mn alloy with and without Sc and Zr calculated by constitutive equation and linear regression method approach the energy of grain boundary diffusion in Al alloy. The activation energy of Al-Mg-Mn-Sc-Zr alloy is lower than that of Al-Mg-Mn alloy. The addition of minor Sc and Zr decreases the activation energy of superplastic deformation.

3) The main mechanism of superplastic deformation of the two alloys is grain boundary sliding accommodated by grain boundary diffusion and dislocation motion. The addition of Sc and Zr refines the microstructure of Al-Mg-Mn alloy. The density of grain boundary in Al-Mg-Mn-Sc-Zr alloy is higher than that in the Al-Mg-Mn alloy; and the finer grain structure and higher density of grain boundary benefit grain boundary sliding. At elevated temperature, dynamic recrystallization brings new fine grains and high angle grain boundaries that benefit grain boundary sliding. Grain boundary diffusion, dislocation motion and dynamic recrystallization in the two alloys harmonize the grain boundary sliding.

## References

- [1] KENDIG K L, MIRACLE D B. Strengthening mechanism of Al-Mg-Sc-Zr alloy [J]. *Acta Materialia*, 2002, 50: 4165–4175.
- [2] YIN Zhi-min, PAN Qing-lin, ZHANG Yong-hong. Effect of trace Sc and Zr on the microstructure and mechanical properties of Al-Mg based alloys [J]. *Materials Science and Engineering A*, 2000, A280: 151–155.
- [3] MILMAN Y V, LOTSKO D V, SIRKO O L. ‘Sc Effect’ of improving mechanical properties in aluminium alloys [J]. *Materials Science Forum*, 2000, 331/337: 1107–1112.
- [4] LATHABAI S, LLOYD P G. The effect of scandium on the microstructure, mechanical properties and weldability of a cast Al-Mg alloy [J]. *Acta Materialia*, 2002, 50: 4275–4292.
- [5] RODER O, WIRTZ T, GYSLER A, LÜTJERING G. Fatigue properties of Al-Mg alloys with and without scandium [J]. *Materials Science and Engineering A*, 1997, A(234/236): 181–184.
- [6] SAITO Y, UTSUNOMIYA H, TSUJI N, SAKAI T. Novel ultra-high straining process for bulk materials development of the accumulative roll-bonding(ARB) process [J]. *Acta Mater*, 1999, 47(2): 579–583.
- [7] GENGA H B, KANGB S B, MIN B K. High temperature tensile behavior of ultra-fine grained Al-3.3Mg-0.2Sc-0.2Zr alloy by equal channel angular pressing [J]. *Materials Science and Engineering A*, 2004, A373: 229–238.
- [8] TURBA K, MÁLEK P, CIESLAR M. Superplasticity in an Al-Mg-Zr-Sc alloy produced by equal-channel angular pressing [J]. *Materials Science and Engineering A*, 2007, A462: 91–94.
- [9] NIEH T G, HSIUNG L M, WADSWORTH J, KAIBYSHEV R. High strain rate superplasticity in a continuously recrystallized Al-6%Mg-0.3%Sc alloy [J]. *Acta Mater*, 1998, 46(8): 2789–2800.
- [10] KAIBYSHEV R, MUSIN F, LESUER D R, NIEH T G. Superplastic behavior of an Al-Mg alloy at elevated temperatures [J]. *Materials Science and Engineering A*, 2003, A342: 169–177.
- [11] MUSIN F, KAIBYSHEV R, MOTOHASHI Y, ITOH G. High strain rate superplasticity in a commercial Al-Mg-Sc alloy [J]. *Scripta Materialia*, 2004, 50: 511–516.
- [12] KAIBYSHEV R, SSKAI T, NIKULIN I, MUSIN F. Achieving superplasticity in the 7055 aluminum alloy [J]. *Materials Science Forum*, 2004, 447/448: 447–452.
- [13] LEE S W, YEH J W. Superplasticity of 5083 alloys with Zr and Mn additions produced by reciprocating extrusion [J]. *Materials Science and Engineering A*, 2007, A460/461: 409–419.
- [14] MANISH C H, I ROY, FARGHALLI A Mohamed. Creep behavior in near-nanostructured Al 5083 alloy [J]. *Materials Science and Engineering A*, 2005, A410/411: 24–27.
- [15] BAE D H, GHOSH A K. Grain size and temperature dependence of superplastic deformation in an Al-Mg alloy under isostructural condition [J]. *Acta Materialia*, 2000, 48: 1207–1224.
- [16] SHERBY O D, WADSWORTH J. Superplasticity—recent advances and future directions [J]. *Progress in Materials Science*, 1989, 33: 169–221.
- [17] WATANABE H, MUKAI T, NIEH T G, HIGASHI K. Low temperature superplasticity in a magnesium-based composite [J]. *Scripta Materialia*, 2000, 42: 249–255.
- [18] CHINH N Q, SZOMMERA P, CSANÁDI T, LANGDON T G. Flow processes at low temperatures in ultrafine-grained aluminum [J]. *Materials Science and Engineering A*, 2006, A434: 326–334.
- [19] PARK K T, HWANG D Y, LEE Y K, KIM Y K, SHIN D H. High strain rate superplasticity of submicrometer grained 5083 Al alloy containing scandium fabricated by severe plastic deformation [J]. *Materials Science and Engineering A*, 2003, A341: 273–281.
- [20] WOO K D, KIM S W, YANG C H, TAI PING LOU, YASUHIRO MIURA. Effects of grain size on high temperature deformation behavior of Al-4Mg-0.4Sc alloy [J]. *Materials Letters*, 2003, 57: 1903–1909.
- [21] WU Shi-dun. Theory of metallic superplastic deformation [M]. Beijing: National Defence Industry Press, 1997: 37.
- [22] TAN J C, TAN M J. Superplasticity and grain boundary sliding characteristics in two stage deformation of Mg-3Al-1Zn alloy sheet [J]. *Materials Science and Engineering A*, 2003, A339: 81–89.
- [23] MA Z Y, MISHRA R S, MAHONEY M W. Superplastic deformation behaviour of friction stir processed 7075Al alloy [J]. *Acta Materialia*, 2002, 50: 4419–4430.

(Edited by YUAN Sai-qian)